Journal of Molecular Catalysis B: Enzymatic 101 (2014) 16–22

Contents lists available at ScienceDirect

Journal of Molecular Catalysis B: Enzymatic

journal homepage: www.elsevier.com/locate/molcatb

Kinetic model for the esterification of ethyl caproate for reaction optimization

Dragana P.C. de Barros*, Fátima Pinto, Luís P. Fonseca, Joaquim M.S. Cabral, F. Lemos

Institute for Biotechnology and Bioengineering, Centre for Biological and Chemical Engineering, Instituto Superior Técnico, 1049-001 Lisbon, Portugal

ARTICLE INFO

Article history:
Received 20 September 2013
Received in revised form
13 December 2013
Accepted 21 December 2013
Available online 29 December 2013

Keywords:
Kinetic model
Enzymatic esterification
Organic solvent
Cutinase
Productivity

ABSTRACT

The present work aims to achieve additional insight on a mechanism describing the fundamental steps involved in the esterification reactions catalyzed by cutinase. The synthesis of ethyl caproate has been used as a model system to obtain a suitable kinetic model to estimate the activation energies involved in the various steps of the reaction pathway.

Kinetic measurements have been made for the enzymatic esterification of caproic acid with ethyl alcohol catalyzed by recombinant *Fusarium solani pisi* cutinase expressed in *Saccharomyces cerevisiae* SU50. Different temperature conditions, from 25 to 50 °C, were tested for two different alcohol/acid molar ratios ($R = 1$ and $R = 2$). The third ordered Ping Pong Bi Bi mechanism with alcohol inhibition was shown to be able to describe the experimental results. The model shows that the productivity decreases as the reaction temperature increases.

1. Introduction

Alkyl esters, an important part of aroma compounds, are commonly used in food, cosmetic and pharmaceutical industries. The use of biocatalysis, using hydrolytic enzymes, for the synthesis of aroma compounds of biological interest has gained a particular interest during the last decades. Advantages of using the enzymatic synthesis in non-aqueous media significantly expand the possibilities for industrial applications [1–3].

There are several reasons for the use of enzymes, mainly lipases and esterases, for the synthesis of short chain acid esters. Enzyme esterification is an interesting option when compared to chemical synthesis as it has the advantages of being able to be carried-out under mild reaction conditions and to ensure the high quality and purity of the products; also have been considered as natural components by food regulatory agencies [4,5].

Fusarium solani pisi (*F.s.pisi*) cutinase activity in hydrolysis, esterification and transesterification has been extensively exploited in recent years and several applications in different industrial fields have been proposed [6]. Numerous report of using cutinases in different reaction media, often dissolved in aqueous solution but also suspended as a powder or immobilized, have been reported [7–18]. Fundamental studies on the hydrolysis of triglycerides [7] clarification of its mechanism regarding stereo-selectivity and specificity [8], and studies of esterification reactions [9–18] were performed with lyophilized cutinase.

The sub-family of cutinases consists of about 20 members, based on amino-acid sequence similarity, which display hydrolytic activity on cutin polymers and efficiently hydrolyze soluble small carboxylic esters and emulsified triacylglycerols.

Cutinase belongs to the family of serine hydrolases containing its catalytic serine centre at the middle of a sharp turn between a β-strand and a α-helix [6]. The catalytic triad, *Ser-120*, *Asp-175* and *His-188*, is accessible to the solvent and can accommodate different substrates. The esterification reaction was shown to follow a Ping-Pong Bi Bi mechanism [15,16]. The serine in the active centre of the enzyme is a very strong nucleophile, which attacks the carbonyl group of the acid (Ac), forming a stable tetrahedral intermediate acyl enzyme complex. The acyl enzyme complex is stabilized by the oxyanion hole. Water is then released and the structure reverts to the planar carbonyl flat plane acyl enzyme intermediate (EA_c). The alcohol (Al) acts afterwards as a new nucleophile and links to the tetrahedral intermediate. Subsequently, as the final step, the resolution of tetrahedral complex yields the ester (Es) and the free enzyme (E).

The industrial application of any chemical reaction requires the knowledge of its kinetics, in particular by using a suitable kinetic model, to allow the description of a chemical reaction and its

* Corresponding author at: Department of Bioengineering, IBB – Institute for Biotechnology and Bioengineering, Centre for Biological and Chemical Engineering, Instituto Superior Técnico, Av. Rovisco Pais, 1049-001, Lisbon, Portugal.
Tel.: +351 218 419 065; fax: +351 218 419 062.
E-mail address: dragana@ist.utl.pt (D.P.C. de Barros).

1381-1177/$ – see front matter © 2014 Elsevier B.V. All rights reserved.
http://dx.doi.org/10.1016/j.molcatb.2013.12.012

Ac	acid
Al	alcohol
Es	ester
E	free enzyme
$[E]_t$	total enzyme concentration, mM
EA_c	enzyme acyl complex
EA_{c2}	enzyme acyl complex with two bound acid molecules
EA_{c3}	enzyme–acyl complex with three bound acid molecules
EA_l	enzyme–alcohol complex
THC	tetrahedral intermediate acyl enzyme complex
$K_{a1}, K_{a2}, K_{a3}, K_{b1}, K_{b1}, K_{b1}$	equilibrium constants
K_i	inhibition coordination constant
$k_{a1}, k_{-a1}, k_{a2}, k_{-a2}, k_{a3}, k_{-a3}, k_{b1}, k_{-b1}, k_{b1}, k_{-b2}, k_{b3}, k_{-b3}$	rate constants, $mM^{-1}\,min^{-1}$

optimization over an extensive range of reagents composition and presence of inhibitors and concentrations, and reaction conditions such as temperature, pH, pressure, etc.

In order to ensure that the model is applicable over a wide range of experimental conditions it should be preferentially based on a mechanistic scheme describing the fundamental steps involved in the reaction. The development of this kind of models can also be used to provide insight into the processes that are taking place.

From previous studies [12,15] *F.s. pisi* cutinase expressed in *Saccharomyces cerevisiae* showed a significant potential for the synthesis of short chain ethyl esters in isooctane. The kinetic parameters of this system in terms of Ping Pong Bi Bi models were estimated, under isothermal conditions, to improve the description of the reaction system. However, the impact of different temperature regimes in the reaction progress is very important and requires additional study. The impact of temperature in the ester yield and rate is difficult to predict because it may affect reaction efficiency in conflicting ways and this knowledge is required for system optimization. On one hand a temperature raise will have a positive effect on the reaction rates, as expected from the transition state theory. On the other hand, higher temperatures may disrupt the enzyme's tertiary structure, causing it to lose its catalytic activity.

Therefore, the aim of this work was evaluation of activation energy of the different steps of the cutinase catalyzed esterification to analyze temperature impact in the production of ethyl caproate.

2. Materials and methods

2.1. Enzyme and chemicals

Caproic acid (C_6) (99.0%, Fluka, Germany) and ethanol abs. (VWR, Germany) were used for ester synthesis, while iso-octane (99.5%, Fluka, Germany) was used as organic solvent and *n*-decane (VWR, Germany) was used as an internal standard for gas chromatography (GC). Sodium sulfate anhydride (Acros, Geel, Belgium) was used to dry iso-octane as organic media of esterification reactions. Saturated salt solution of sodium chloride (Panreac, Spain) was used to control water activities of enzyme and substrates. All other chemicals used were of analytical grade.

Fusarium solani pisi cutinase wild-type was biosynthesized by recombinant *S. cerevisiae* SU50 strain as described by Calado et al. [19]. The isolation and purification and characterization of cutinase excreted by recombinant *S. cerevisiae* SU50 strain was carried out by according to previous published protocols [12,15]. Lyophilized pure cutinase was stored at −20 °C before used in esterification reactions. Activities of lyophilized cutinase preparations were of $240 \pm 10\,U\,m^{-1}$ of reaction medium according the p-NPB method [11].

Table 1
Experimental conditions for the set of experiments used in the fitting of the different models.

T, °C	Al/Ac = 1		Al/Ac = 2	
	Ethanol, mM	Caproic acid, mM	Ethanol, mM	Caproic acid, mM
25	208	205	217	121
30	231	214	210	117
35	211	199	210	110
40	216	219	204	114
45	214	213	203	119
50	213	197	210	117

All concentrations are given in mM. Enzyme concentration is equal to 0.1 mM in all runs and the specific activity was $240 \pm 10\,U\,ml^{-1}$ of reaction media.

2.2. Enzymatic esterification

The esterification of acid and alcohol by cutinase was carried out in iso-octane as organic solvent, as previously explained [15]. The enzymatic ester synthesis was performed in an incubator (AGITORB 16OE, Aralab, Portugal) at various temperatures (25–50 °C), and cutinase concentration of 2 mg/ml of reaction mixture. Experiments were performed at least in duplicate and the experimental error was estimated less than 8%. Samples were withdrawn periodically using a needle, without destroying the rubber cap, and analyzed by GC. The reaction yield was calculated according to the molar ratio between the ethyl ester and respective limiting substrate, in this case acid.

2.3. Methods for monitoring substrate and ester concentrations

The concentrations of ethanol, caproic acid and ethyl caproate were determined using a Hewlett–Packard model 5890 gas chromatograph, equipped with a flame ionization detector (FID). A WCOT Fused Silica coating CP Chirasil-Dex CB column, 25 m × 0.25 mm, DF = 0.25 (Varian Inc.) was used to separate the components in the reaction mixture. *n*-Decane was used as an internal standard in the quantification of ethyl esters and respective substrates concentrations in the reaction media. Nitrogen was used as carrier gas. The oven temperature was held at 50 °C for 4 min before being raised to 160 °C for 1.67 min at 15 °C min^{-1}; the injector temperature was set at 200 °C and the detector temperature was set at 250 °C.

2.4. Kinetic model

The base model development was described in a previous work [15] where it was applied to data at a single temperature. To implement the different models the appropriate differential and equilibrium equations were written for each kinetic model and an approximate global reaction rate was obtained using the quasi-steady-state approximation. This rate equation was used to compute the time-course evolution of the different species involved by numerical integration of the material balances using the Euler method.

The model was fitted to the experimental data (all the available experiments were used simultaneously) by a least squares procedure where the objective function consisted of the sum of the square of relative errors of the ethanol, caproic acid and ethyl caproate concentrations measured in all experiments. The experimental conditions, for the set of experiments used in fitting procedure are given in Table 1. This procedure was carried-out using a Microsoft Excel 2003 spreadsheet and the estimation of the

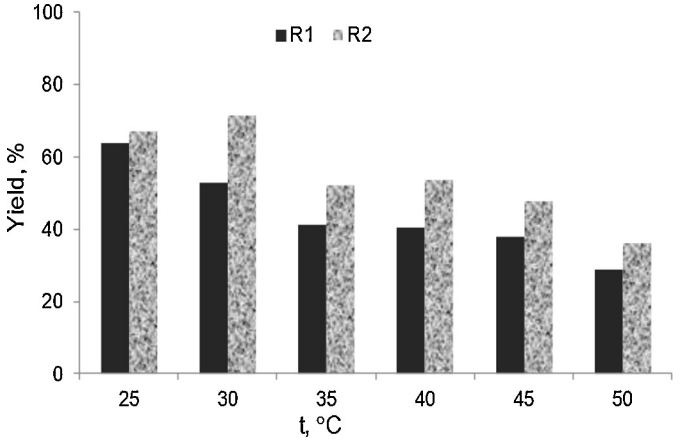

Fig. 1. Effect of the temperature on esterification yield for alcohol/acid molar ratio $R1 = 1$ and $R2 = 2$ (ethanol = 0.2 M) at the end of the reaction (6 h).

parameters was carried-out using the Solver tool, as in the previous work [15].

3. Results and discussion

3.1. Effect of temperature

The effect of temperature on esterification yield was observed for two different alcohol/acid molar ratios ($R = 1$ and $R = 2$), for temperature range from 25 °C to 50 °C, with increment of 5 °C (Fig. 1).

A different yield profile was observed for two different molar ratios. In the case of the $R = 1$ the ester yield decrease with the temperature raise from 25 to 50 °C. For molar ratio $R = 2$, esterification yield increase from 67% to 71%) if temperature increased from 25 to 30 °C and then a significant yield decay was observed for temperature above 30 °C (52% for 35 °C).

Lower esterification yield observed for $R = 1$, independently of the temperature value, may be due to the alcohol inhibitory effect already observed by previous work [12].

3.2. Base kinetic model

The esterification of caproic acid with ethanol was catalyzed by cutinase *F.s. pisi* in iso-octane.

$$\mathrm{Ac} + \mathrm{Al} = \mathrm{Es} + \mathrm{H_2O} \tag{1}$$

The accepted mechanism for this reaction Ping-Pong Bi-Bi kinetic mechanism with inhibition by the substrates [15] was taken as the basis for the reaction esterification of caproic acid by ethanol catalyzed by cutinase (Eq. (1)). Taking into consideration that for this reaction it is essential that an acyl–enzyme bond is formed, the first step will be the formation of the active enzyme–acyl complex between cutinase and the caproic acid and the second step will be reaction of the enzyme–acyl complex with the alcohol end ester formation. Following the procedure used in the previous work [15] the rate limiting step approximation was applied. The reaction rate will be limited by the rate of the second reaction. The model was further extended to consider that up to three acid molecules could bind to the enzyme (Eqs. (2)–(7)), following previous observations, where it was observed that for the hydrolysis of triglycerides, the enzyme was able to bind up to 3 of products molecules [20].

$$\mathrm{E} + \mathrm{Ac} \rightleftharpoons \mathrm{EA_c} + \mathrm{H_2O} \quad K_{a_1} = \frac{k_{a_1}}{k_{-a_1}} \tag{2}$$

$$\mathrm{EA_c} + \mathrm{Al} \rightleftharpoons \mathrm{E} + \mathrm{Es} \quad K_{b_1} = \frac{k_{b_1}}{k_{-b_1}} \tag{3}$$

$$\mathrm{EA_c} + \mathrm{Ac} \rightleftharpoons \mathrm{EA_{c2}} + \mathrm{H_2O} \quad K_{a_2} = \frac{k_{a_2}}{k_{-a_2}} \tag{4}$$

$$\mathrm{EA_{c2}} + \mathrm{Al} \rightleftharpoons \mathrm{EA_c} + \mathrm{Es} \quad K_{b_2} = \frac{k_{b_2}}{k_{-b_2}} \tag{5}$$

$$\mathrm{EA_{c2}} + \mathrm{Ac} \rightleftharpoons \mathrm{EA_{c3}} + \mathrm{H_2O} \quad K_{a_3} = \frac{k_{a_3}}{k_{-a_3}} \tag{6}$$

$$\mathrm{EA_{c3}} + \mathrm{Al} \rightleftharpoons \mathrm{EA_{c2}} + \mathrm{Es} \quad K_{b_3} = \frac{k_{b_3}}{k_{-b_3}} \tag{7}$$

$$[\mathrm{E}]_\mathrm{t} = [\mathrm{E}] + [\mathrm{EA_c}] + [\mathrm{EA_{c2}}] + [\mathrm{EA_{c3}}] \tag{8}$$

Given that all reactions were carried-out in closed vessels we have considered that the evaporation of all the components in the mixture is negligible, the volume was considered to be constant. With this assumption the material balances for a batch reactor, for all the species involved, can be described by the following set of differential equations:

$$\frac{d[\mathrm{E}]}{dt} = -k_{a_1}[\mathrm{E}][\mathrm{Ac}] + k_{-a_1}[\mathrm{EA_c}][\mathrm{H_2O}] + k_{b_1}[\mathrm{EA_c}][\mathrm{Al}] - k_{-b_1}[\mathrm{E}][\mathrm{Es}] \tag{9}$$

$$\frac{d[\mathrm{Ac}]}{dt} = -k_{a_1}[\mathrm{E}][\mathrm{Ac}] + k_{-a_1}[\mathrm{EA_c}][\mathrm{H_2O}] \tag{10}$$

$$\frac{d[\mathrm{H_2O}]}{dt} = k_{a_1}[\mathrm{E}][\mathrm{Ac}] - k_{-a_1}[\mathrm{EA_c}][\mathrm{H_2O}] \tag{11}$$

$$\frac{d[\mathrm{Al}]}{dt} = -k_{b_1}[\mathrm{EA_c}][\mathrm{Al}] + k_{-b_1}[\mathrm{E}][\mathrm{Es}] \tag{12}$$

$$\frac{d[\mathrm{Es}]}{dt} = k_{b_1}[\mathrm{EA_c}][\mathrm{Al}] - k_{-b_1}[\mathrm{E}][\mathrm{Es}] \tag{13}$$

$$\frac{d[\mathrm{EA_c}]}{dt} = k_{a_1}[\mathrm{E}][\mathrm{Ac}] - k_{-a_1}[\mathrm{EA_c}][\mathrm{H_2O}] - k_{b_1}[\mathrm{Ac}][\mathrm{Al}] + k_{-b_1}[\mathrm{E}][\mathrm{Es}] \tag{14}$$

Combining all these equations and assuming that the quasi stationary state assumption can be applied for, Eqs. (9) and (14), the global reaction rates for the first, second and third order, respectively, for the systems without inhibition were obtained as it was described in a previous work [15]:

All of these schemes were changed so as to incorporate the possibility of reversible inhibition by the alcohol binding to the enzyme site (Eq. (15)) and adequate reaction rate equation is given by Eq. (16):

$$\mathrm{E} + \mathrm{Al} = \mathrm{EA_l} \tag{15}$$

$$[\mathrm{EA_l}] = K_i[\mathrm{E}][\mathrm{Al}]$$

$$r = \frac{k_{b_1}[\mathrm{E}]_\mathrm{t}((K_{a_1}(([\mathrm{Ac}][\mathrm{Al}])/[\mathrm{H_2O}]) - [\mathrm{Es}])/K_{b_1}) + \cdots}{1 + K_i[\mathrm{Al}] + K_{a_1}([\mathrm{Ac}]/\mathrm{H_2O}) + \cdots} \tag{16}$$

A total enzyme amount is given by expression:

$$[\mathrm{E}]_\mathrm{t} = [\mathrm{E}] + [\mathrm{EA_c}] + [\mathrm{EA_{c2}}] + [\mathrm{EA_{c3}}] + [\mathrm{EA_l}] \tag{17}$$

Table 2
Values of kinetic and equilibrium constants with and without alcohol inhibition for the thermodynamically consistent model.

Constant	Order					
	1st	2nd	3rd	$1st_i$	$2nd_i$	$3rd_i$
K_{a1}	1.54E+05	2.31E+04	2.42E+04	4.72E+04	2.39E+04	2.14E+04
K_{a2}	–	8.14E−02	4.14E−11	–	3.62E−02	2.51E+00
K_{a3}	–	–	1.55E+08	–	–	1.01E+00
K_{b1}	1.07E−05	7.63E−05	7.24E−05	3.48E−05	9.34E−05	1.24E−03
K_{b2}	–	2.16E+01	4.23E+10	–	6.25E+01	1.06E+01
K_{b3}	–	–	1.13E−08	–	–	2.30E+01
k_{b1}	4.41E−02	5.62E−02	5.58E−02	4.41E−02	5.47E−02	5.71E−01
k_{b2}	–	2.55E−02	1.45E+00	–	3.27E−02	4.32E−01
k_{b3}	–	–	2.54E−02	–	–	1.67E−02
K_i	–	–	–	1.33E−08	1.07E+02	2.12E+04
F_{obj}	33 366	26 869	26 704	33 349	24 197	20 097

1st, 2nd, 3rd – without alcohol inhibition, $1st_i$, $2nd_i$, $3rd_i$ – with alcohol inhibition.
Rate constants unites k_{b1}, k_{b2}, k_{b3} are $mM^{-1}\ min^{-1}$.

The dependence of rates on temperature manifests in the temperature dependence of the rate constant k_i.

$$k_i = k(t_i), \quad t_i = 25\,^{\circ}C, \quad 30\,^{\circ}C, \quad 35\,^{\circ}C, \quad 40\,^{\circ}C, \quad 45\,^{\circ}C, \quad 50\,^{\circ}C \tag{18}$$

The quantitative relationship between the rate constant and temperature was expressed by the Arrhenius equation, written as:

$$k_i = k_{ref} \exp\left[\frac{E_A}{R}\left(\frac{1}{T_i} - \frac{1}{T_{ref}}\right)\right] \tag{19}$$

where k_{ref}, represent the kinetic constant at a reference temperature $T_{ref} = 303.17$ K, $T_i = 273.17 + t_i$ and R is the universal gas constant.

By application of van't Hoff equation the relationship between the equilibrium constants K_{a_j} and K_{b_j} with the apparent standard enthalpy change ΔH_{a_j} and ΔH_{b_j} ($j = 1, 2, 3$ present reaction order).

$$K_{a_j,b_j} = K_{ref} \exp\left[\frac{\Delta H_{a_j,b_j}}{R}\left(\frac{1}{T_i} - \frac{1}{T_{ref}}\right)\right] \tag{20}$$

where K_{ref}, represent the equilibrium constant at a reference temperature $T_{ref} = 303.17$ K, $T_i = 273.17 + t_i$ ($t_i = 25, 30, 35, 40, 45, 50\,^{\circ}C$) and R is the universal gas constant.

The model was solved for all experimental conditions that were used, as explained above. The consistency between chemical kinetic and thermodynamics plays an important role (Eq. (21)) [21]. So, the refinement of the third order model with alcohol inhibition was performed and the equilibrium constant and rate constant was obtained.

$$K_{a_1}K_{b_1} = K_{a_2}K_{b_2} = K_{a_3}K_{b_3} \tag{21}$$

The third order model with alcohol inhibition was confirmed to provide a better description of the experimental results, as shown by the fact that its objective function (F_{obj}) decreases by rise of the reaction order and inclusion of the alcohol inhibition (Table 2) and it was used to study the temperature influence for two different molar ratios. The estimated kinetic parameters for all models that were tested are shown in Table 2.

K_{a1}, K_{a2}, K_{a3}, K_{b1}, K_{b2}, K_{b3}, K_i are equilibrium constants and k_{b1}, k_{b2}, k_{b3} are rate constants. The rate limiting approximation does not allow the simultaneous estimation of k_a and k_{-a}, since the first step is considered to be in equilibrium.

It was observed (Table 2) that the inclusion of higher order coordination of the acid molecules for the systems without inhibition improve the description of the experimental data only for 2nd order model (decrease the F_{obj} 19.5%), but further order increase did not improve significantly the data description (less than 1%).

On the other hand inclusion of inhibition for the 1st order model does not produce any significant improvement in description of the experimental data but nevertheless influence of the inhibition effect for the 2nd order model (F_{obj} reduce 10%) and specially for the 3rd order model (F_{obj} reduce 25%) is significant. In models with inhibition the higher positive impact of the high order inclusion was observed too. F_{obj} from 1st to 2nd order model reduce 27% and from 2nd to 3rd order 17%.

The apparent equilibrium constant for the 3rd ordered model with inhibition $K_{a1} > K_{a2} > K_{a3}$, which indicates that enzyme is much less receptive for the binding of a second and third acid molecules. The binding affinity of second and third acid molecule is quite similar.

The kinetic model indicates that all the species with bound substrate molecules are active for the synthesis reaction and with kinetic rate constants that decrease as the number of substrate molecules bound increases, as it can be seen by the order $k_{b1} > k_{b2} > k_{b3}$ in Table 2.

Inclusion of alcohol inhibition shows important improvement on the quality of fitting obtained, so we can conclude that the change in the temperature regime, studied in this work, underlines more alcohol inhibition then it was the case with isothermic system observed by previous work [15].

Table 3 summarizes the values of activation energies and enthalpies for the 3rd ordered reaction with alcohol inhibition systems, obtained from the Eq. (19) and Eq. (20).

An evaluation of the error on the estimated kinetic parameters was obtained using a "bootstrap technique" [22]. In this procedure, 1/3 of original data points were randomly replaced by other data points in the same set and a new optimization procedure was performed. This procedure was repeated 20 times and the reported set

Table 3
Kinetic constants, enthalpies and activation energies for the 3rd ordered reaction with alcohol inhibition systems ($3rd_i$).

Constants		Energies, kJ mol^{-1}	
K_{a1}	(21.4 ± 1.78)E+03	ΔH_{a_1}	−141 ± 3.88
K_{a2}	(2.51 ± 0.313)E+00	ΔH_{a_2}	−494 ± 11.4
K_{a3}	(1.01 ± 0.552)E+00	ΔH_{a_3}	−672 ± 16.0
K_{b1}	(1.24 ± 0.723)E−03	ΔH_{b_1}	−70 ± 9.19
K_{b2}	(1.06 ± 0.248)E+01	ΔH_{b_2}	0
K_{b3}	(2.30 ± 1.56)E+01	ΔH_{b_3}	−527 ± 21.3
k_{b1}	(0.571 ± 0.338)E+00	ΔE_{b1}	182 ± 11.8
k_{b2}	(4.32 ± 0.447)E−01	ΔE_{b2}	149 ± 15.4
k_{b3}	(1.67 ± 0.264)E−03	ΔE_{b3}	48 ± 11.2
K_i	(2.12 ± 0.431)E+04	ΔH_i	−26 ± 12.6

Rate constants unites k_{b1}, k_{b2}, k_{b3} are $mM^{-1}\ min^{-1}$.

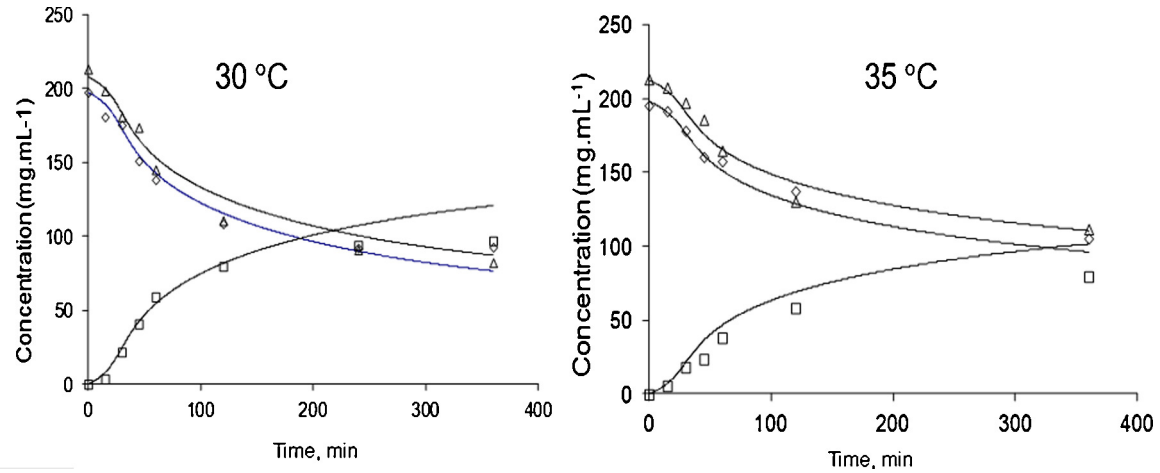

Fig. 2. Experimental results for alcohol/acid molar ratio $R = 1$, [Alcohol] = 200 mM. Ethanol (*triangle*), caproic acid (*diamond*), ethyl caproate (*square*). Lines correspond to the kinetic model.

of parameters, for a 90% confidence level, was computed from the distribution of parameter values obtained. Table 3 summarizes the values of kinetic constants, activation energies and enthalpies for the 3rd ordered reaction with alcohol inhibition systems.

The values of apparent enthalpy change for the formation of enzyme–acyl complex ΔH_{a_j} show favourable energies for the binding of 3rd acid molecule.

The results have shown that the overall reaction rate increases with temperature, resulting in apparent positive overall activation energy.

It should, however, be noted that the parameters obtained cannot be viewed as true kinetic or thermodynamic parameters but they only describe the mechanistic approach that was used. Nevertheless the results obtained describe with very good accuracy the experimental results and can be used with confidence within the range of experimental conditions that was covered by this study.

To check for the extrapolation capabilities of the model obtained, it was used on a different set of experimental data without further optimization of the model parameters.

3.3. Evaluation of the model fitting to the experimental data

The quality of fittings was checked by looking at 6 series of experiments that were carried out at different temperature, 30, 35, 40 and 45 °C testing two molar alcohol/acid (R) molar ratio: $R = 1$ (Fig. 2) and $R = 2$ (Fig. 3).

A set of experimental data for molar ratio $R = 1$ is depicted in Fig. 2.

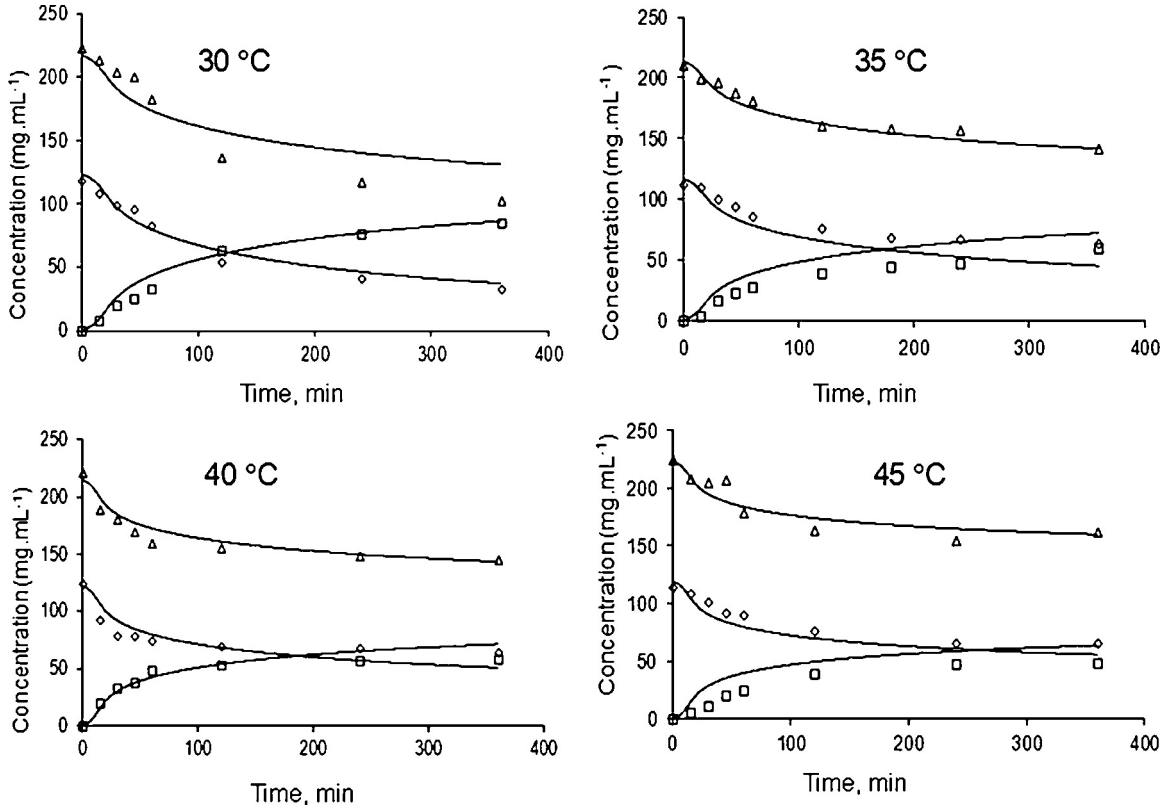

Fig. 3. Experimental results for alcohol/acid molar ratio $R = 2$, [Alcohol] = 200 mM. Ethanol (*triangle*), caproic acid (*diamond*), ethyl caproate (*square*). Lines correspond to the kinetic model.

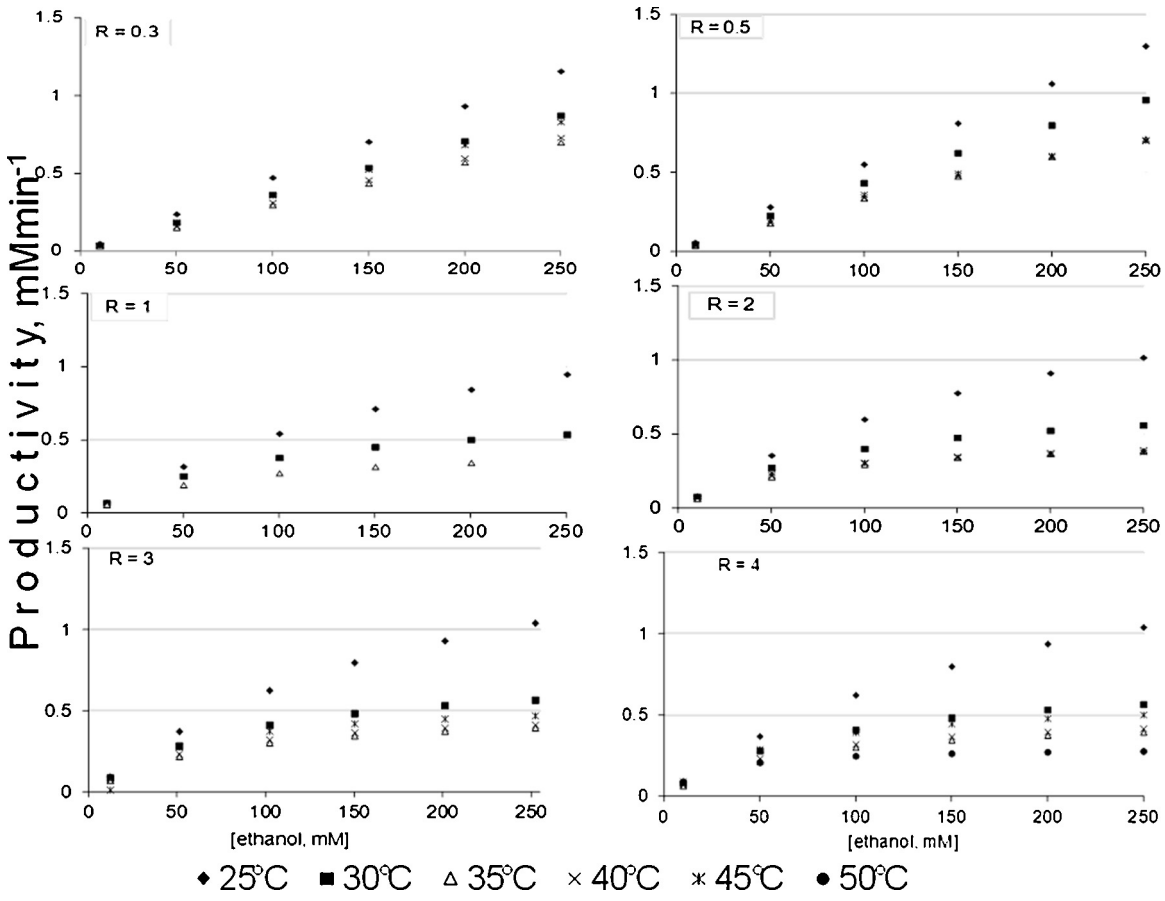

Fig. 4. Productivity for the systems with different alcohol/acid molar ratio for temperature range 25–50 °C.

A very good quality of the model was obtain for the molar ratio $R = 1$ (Fig. 2). The higher prediction esterification yield, observed in the model for the reaction time above 2 h, may be due to the inhibition effects of the substrates during the time course of the reaction, already observed by previous work of the authors [12,15].

The prediction quality of the esterification yield was improved for the molar ratio $R = 2$ (Fig. 3).

As it can be seen the model was able to describe the experimental data within a good margin of accuracy.

3.4. Optimization of the system

The model was applied for different alcohol/acid molar ratio ($R = 0.3$; 0.5; 1, 2, 3 and 4, respectively) in all temperature range (25–50 °C), for the initial alcohol concentration from 10 to 250 mM, and the time when esterification yield reaches 50% of equilibrium value was observed (Fig. 4).

The model shows that productivity decreases as the temperature increases for all alcohol/acid molar ratios. The fall in productivity is specially emphasized for high alcohol concentrations (Table 4). For the initial alcohol concentration of 250 mM and for molar ratios $R = 3$ and $R = 4$ the productivity declines to 45.5%, and for $R = 0.3$ the productivity decreases to 25%.

It means that lower temperatures favour the reaction esterification, and the alcohol inhibition has significant influence on the productivity.

Table 4
Difference in productivity (mM min^{-1}), for temperature increase from 25 to 30 °C for different alcohol/acid molar ratio.

[Al], mM	R					
	0.3	0.5	1	2	3	4
50	0.054	0.055	0.065	0.083	0.089	0.090
150	0.166	0.188	0.261	0.301	0.314	0.316
250	0.285	0.341	0.412	0.458	0.474	0.473

4. Conclusions

From the results presented and the fittings obtained we can conclude that the kinetic of synthesis of ethyl caproate catalyzed by cutinase follows a complex scheme and that, as previously observed, the cutinase can bind up to three substrate molecules. The results also indicate, as expected, that alcohol inhibits the reaction. Although we cannot conclude that all three bound acid molecules can be activated, the kinetic model indicates that all the species with bound substrate molecules are active for the synthesis reaction and with kinetic rate constants that decrease as the number of substrate molecules bound increases, as it can be seen by the order $k_{b1} > k_{b2} > k_{b3}$ in Table 3.

The development of a kinetic model has enabled us to analyze the impact of the various operating parameters in the production of ethyl caproate and conclude that the reaction is better carried-out a low temperature.

Acknowledgement

Dragana P.C. de Barros acknowledges Fundação para a Ciência e a Tecnologia (Portugal) for financial support in the form of the grant SFRH/BPD/70409/2010.

References

[1] J. Schrader, M.M.W. Etschmann, D. Sell, J.-M. Hilmer, J. Rabenhorst, Biotechnol. Lett. 26 (2004) 463–472.
[2] J.P. Rasor, E. Voss, Appl. Catal. A: Gen. 221 (2001) 145–158.
[3] E.J. Vandamme, W. Soetaert, J. Chem. Technol. Biotechnol. 77 (2002) 1323–1332.
[4] A. Schmid, J.S. Dordick, B. Hauer, A. Kiener, M. Wubbolts, B. Witholt, Nature 409 (2001) 258–268.
[5] S. Hari-Krishna, N.G. Karanth, Catal. Rev. 44 (2002) 499–591.
[6] C.M.L. Carvalho, M.R. Aires-Barros, J.M.S. Cabral, Biotechnol. Bioeng. 66 (1999) 17–34.
[7] J.A.C. Flipsen, H.T.W.M. van der Hijden, M.R. Egmond, H.M. Verheij, Chem. Phys. Lipids 84 (1996) 105–115.
[8] M.L.M. Mannesse, R.C. Cox, B.C. Koops, H.M. Verheij, G.H. Haas, M.R. Egmond, et al., Biochemistry 34 (1995) 6400–6407.
[9] C. Sarazin, F. Ergan, J.P. Séguin, G. Goethals, M.D. Legoy, J.N. Barbotin, Biotechnol. Bioeng. 51 (1995) 636–644.
[10] A.M. Pinto-Sousa, J.M.S. Cabral, M.R. Aires-Barros, Biocatalysis 9 (1994) 169–179.
[11] D.P.C. de Barros, L.P. Fonseca, J.M.S. Cabral, C.K. Weiss, K. Landfester, Biotechnol. J. 4 (2009) 674–683.
[12] D.P.C. de Barros, L.P. Fonseca, P. Fernandes, J.M.S. Cabral, L.j. Mojovic, J. Mol. Catal. B: Enzyme 60 (2009) 178–185.
[13] D.P.C. de Barros, L.P. Fonseca, J.M.S. Cabral, E.M. Aschenbrenner, C.K. Weiss, K. Landfester, Biotechnol. Bioeng. 106 (2010) 507–515.
[14] D.P.C. de Barros, P. Fernandes, J.M.S. Cabral, L.P. Fonseca, J. Chem. Technol. Biotechnol. 85 (2010) 1553–1560.
[15] D.P.C. de Barros, F. Lemos, L.P. Fonseca, J.M.S. Cabral, J. Mol. Catal. B: Enzyme 66 (2010) 285–293.
[16] F.N. Serralha, J.M. Lopes, F. Lemos, D.M.F. Prazeres, M.R. Aires-Barros, J.M.S. Cabral, F. Ramôa Ribeiro, J. Mol. Catal. B: Enzyme 11 (2001) 713–718.
[17] D.P.C. de Barros, P. Fernandes, J.M.S. Cabral, L.P. Fonseca, Catal. Today 173 (2011) 95–102.
[18] D.P.C. de Barros, A.M. Azevedo, J.M.S. Cabral, L.P. Fonseca, J. Food Biochem. 36 (2012) 275–284.
[19] C.R.C. Calado, C. Almeida, J.M.S. Cabral, L.P. Fonseca, J. Biosci. Bioeng. 96 (2003) 141–148.
[20] D.M.F. Prazeres, F. Lemos, F.A.P. Garcia, J.M.S. Cabral, Biotechnol. Bioeng. 42 (1993) 759–764.
[21] G. Jenkinson, J. Goutsias, BMC Syst. Biol. 5 (2011) 1–13.
[22] W.H. Press, S.A. Teukolsky, W.T. Vetterling, B.P. Flannery, Numerical Recipes in C: The Art of Scientific Computing, second ed., Cambridge University Press, Cambridge, 1992, pp. 684.